Anthropogenic emissions of methane in the United States

Scot M. Miller[a,1], Steven C. Wofsy[a], Anna M. Michalak[b], Eric A. Kort[c], Arlyn E. Andrews[d], Sebastien C. Biraud[e], Edward J. Dlugokencky[d], Janusz Eluszkiewicz[f], Marc L. Fischer[g], Greet Janssens-Maenhout[h], Ben R. Miller[i], John B. Miller[i], Stephen A. Montzka[d], Thomas Nehrkorn[f], and Colm Sweeney[i]

[a]Department of Earth and Planetary Sciences, Harvard University, Cambridge, MA 02138; [b]Department of Global Ecology, Carnegie Institution for Science, Stanford, CA 94305; [c]Department of Atmospheric, Ocean, and Space Sciences, University of Michigan, Ann Arbor, MI 48109; [d]Global Monitoring Division, Earth System Research Laboratory, National Oceanic and Atmospheric Administration, Boulder, CO 80305; [e]Earth Sciences Division, and [g]Environmental Energy Technologies Division, Lawrence Berkeley National Laboratory, Berkeley, CA 94720; [f]Atmospheric and Environmental Research, Lexington, MA 02421; [h]Institute for Environment and Sustainability, European Commission Joint Research Centre, 21027 Ispra, Italy; and [i]Cooperative Institute for Research in Environmental Sciences, University of Colorado Boulder, Boulder, CO 80309

This study quantitatively estimates the spatial distribution of anthropogenic methane sources in the United States by combining comprehensive atmospheric methane observations, extensive spatial datasets, and a high-resolution atmospheric transport model. Results show that current inventories from the US Environmental Protection Agency (EPA) and the Emissions Database for Global Atmospheric Research underestimate methane emissions nationally by a factor of ~1.5 and ~1.7, respectively. Our study indicates that emissions due to ruminants and manure are up to twice the magnitude of existing inventories. In addition, the discrepancy in methane source estimates is particularly pronounced in the south-central United States, where we find total emissions are ~2.7 times greater than in most inventories and account for 24 ± 3% of national emissions. The spatial patterns of our emission fluxes and observed methane–propane correlations indicate that fossil fuel extraction and refining are major contributors (45 ± 13%) in the south-central United States. This result suggests that regional methane emissions due to fossil fuel extraction and processing could be 4.9 ± 2.6 times larger than in EDGAR, the most comprehensive global methane inventory. These results cast doubt on the US EPA's recent decision to downscale its estimate of national natural gas emissions by 25–30%. Overall, we conclude that methane emissions associated with both the animal husbandry and fossil fuel industries have larger greenhouse gas impacts than indicated by existing inventories.

climate change policy | geostatistical inverse modeling

Methane (CH_4) is the second most important anthropogenic greenhouse gas, with approximately one third the total radiative forcing of carbon dioxide (1). CH_4 also enhances the formation of surface ozone in populated areas, and thus higher global concentrations of CH_4 may significantly increase ground-level ozone in the Northern Hemisphere (2). Furthermore, methane affects the ability of the atmosphere to oxidize other pollutants and plays a role in water formation within the stratosphere (3).

Atmospheric concentrations of CH_4 [~1,800 parts per billion (ppb)] are currently much higher than preindustrial levels (~680–715 ppb) (1, 4). The global atmospheric burden started to rise rapidly in the 18th century and paused in the 1990s. Methane levels began to increase again more recently, potentially from a combination of increased anthropogenic and/or tropical wetland emissions (5–7). Debate continues, however, over the causes behind these recent trends (7, 8).

Anthropogenic emissions account for 50–65% of the global CH_4 budget of ~395–427 teragrams of carbon per year ($TgC·y^{-1}$) (526–569 Tg CH_4) (7, 9). The US Environmental Protection Agency (EPA) estimates the principal anthropogenic sources in the United States to be (in order of importance) (*i*) livestock (enteric fermentation and manure management), (*ii*) natural gas

production and distribution, (*iii*) landfills, and (*iv*) coal mining (10). EPA assesses human-associated emissions in the United States in 2008 at 22.1 TgC, roughly 5% of global emissions (10).

The amount of anthropogenic CH_4 emissions in the US and attributions by sector and region are controversial (Fig. 1). Bottom-up inventories from US EPA and the Emissions Database for Global Atmospheric Research (EDGAR) give totals ranging from 19.6 to 30 $TgC·y^{-1}$ (10, 11). The most recent EPA and EDGAR inventories report lower US anthropogenic emissions compared with previous versions (decreased by 10% and 35%, respectively) (10, 12); this change primarily reflects lower, revised emissions estimates from natural gas and coal production Fig. S1. However, recent analysis of CH_4 data from aircraft estimates a higher budget of 32.4 ± 4.5 $TgC·y^{-1}$ for 2004 (13). Furthermore, atmospheric observations indicate higher emissions in natural gas production areas (14–16); a steady 20-y increase in the number of US wells and newly-adopted horizontal drilling techniques may have further increased emissions in these regions (17, 18).

These disparities among bottom-up and top-down studies suggest much greater uncertainty in emissions than typically reported. For example, EPA cites an uncertainty of only ±13% for the for United States (10). Independent assessments of bottom-up inventories give error ranges of 50–100% (19, 20), and

---

Significance

Successful regulation of greenhouse gas emissions requires knowledge of current methane emission sources. Existing state regulations in California and Massachusetts require ~15% greenhouse gas emissions reductions from current levels by 2020. However, government estimates for total US methane emissions may be biased by 50%, and estimates of individual source sectors are even more uncertain. This study uses atmospheric methane observations to reduce this level of uncertainty. We find greenhouse gas emissions from agriculture and fossil fuel extraction and processing (i.e., oil and/or natural gas) are likely a factor of two or greater than cited in existing studies. Effective national and state greenhouse gas reduction strategies may be difficult to develop without appropriate estimates of methane emissions from these source sectors.
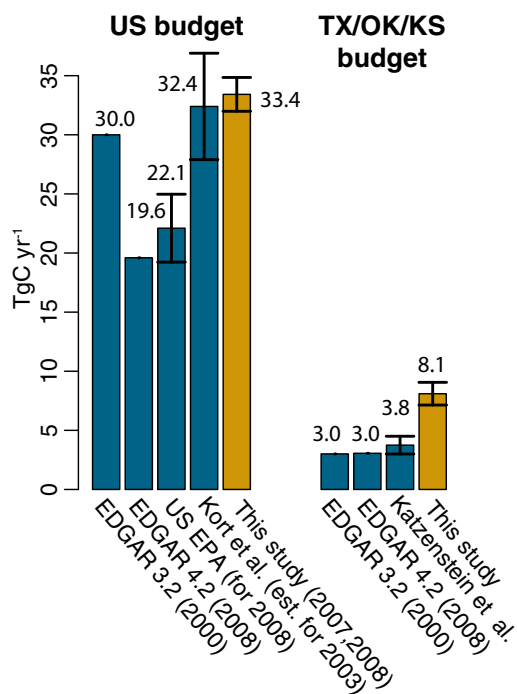

Fig. 1. US anthropogenic methane budgets from this study, from previous top-down estimates, and from existing emissions inventories. The south-central United States includes Texas, Oklahoma, and Kansas. US EPA estimates only national, not regional, emissions budgets. Furthermore, national budget estimates from EDGAR, EPA, and Kort et al. (13) include Alaska and Hawaii whereas this study does not.

values from Kort et al. are $47 \pm 20\%$ higher than EPA (13). Assessments of CH_4 sources to inform policy (e.g., regulating emissions or managing energy resources) require more accurate, verified estimates for the United States.

This study estimates anthropogenic CH_4 emissions over the United States for 2007 and 2008 using comprehensive CH_4 observations at the surface, on telecommunications towers, and from aircraft, combined with an atmospheric transport model and a geostatistical inverse modeling (GIM) framework. We use auxiliary spatial data (e.g., on population density and economic activity) and leverage concurrent measurements of alkanes to help attribute emissions to specific economic sectors. The work provides spatially resolved CH_4 emissions estimates and associated uncertainties, as well as information by source sector, both previously unavailable.

Model and Observation Framework

We use the Stochastic Time-Inverted Lagrangian Transport model (STILT) to calculate the transport of CH_4 from emission points at the ground to measurement locations in the atmosphere (21). STILT follows an ensemble of particles backward in time, starting from each observation site, using wind fields and turbulence modeled by the Weather Research and Forecasting (WRF) model (22). STILT derives an influence function ("footprint," units: ppb CH_4 per unit emission flux) linking upwind emissions to each measurement. Inputs of CH_4 from surface sources along the ensemble of back-trajectories are averaged to compute the CH_4 concentration for comparison with each observation.

We use observations for 2007 and 2008 from diverse locations and measurement platforms. The principal observations derive from daily flask samples on tall towers (4,984 total observations) and vertical profiles from aircraft (7,710 observations). Tower-based observations are collected as part of the National Oceanic and Atmospheric (NOAA)/Department of Energy (DOE)

cooperative air sampling network, and aircraft-based data are obtained from regular NOAA flights (23), regular DOE flights (24), and from the Stratosphere-Troposphere Analyses of Regional Transport 2008 (START08) aircraft campaign (25); all data are publicly available from NOAA and DOE. These observations are displayed in Fig. 2 and discussed further in the *SI Text* (e.g., Fig. S2). We use a GIM framework (26, 27) to analyze the footprints for each of the 12,694 observations, and these footprints vary by site and with wind conditions. In aggregate, the footprints provide spatially resolved coverage of most of the continental United States, except the southeast coastal region (Fig. S3).

The GIM framework, using footprints and concentration measurements, optimizes CH_4 sources separately for each month of 2007 and 2008 on a $1° \times 1°$ latitude–longitude grid for the United States. The contributions of fluxes from natural wetlands are modeled first and subtracted from the observed CH_4 (2.0 TgC·y^{-1} for the continental United States); these fluxes are much smaller than anthropogenic sources in the United States and thus would be difficult to independently constrain from atmospheric data (*SI Text*).

The GIM framework represents the flux distribution for each month using a deterministic spatial model plus a stochastic spatially correlated residual, both estimated from the atmospheric observations. The deterministic component is given by a weighted linear combination of spatial activity data from the EDGAR 4.2 inventory; these datasets include any economic or demographic data that may predict the distribution of CH_4 emissions (e.g., gas production, human and ruminant population densities, etc.). Both the selection of the activity datasets to be retained in the model and the associated weights (emission factors) are optimized to best match observed CH_4 concentrations. Initially, seven activity datasets are included from EDGAR 4.2, (*i*) population, (*ii*) electricity production from power plants, (*iii*) ruminant population count, (*iv*) oil and conventional gas production, (*v*) oil refinery production, (*vi*) rice production, and (*vii*) coal production.

We select the minimum number of datasets with the greatest predictive ability using the Bayesian Information Criterion (BIC) (*SI Text*) (28). BIC numerically scores all combinations of available datasets based on how well they improve goodness of fit and applies a penalty that increases with the number of datasets retained.

The stochastic component represents sources that do not fit the spatial patterns of the activity data (Fig. S4). GIM uses
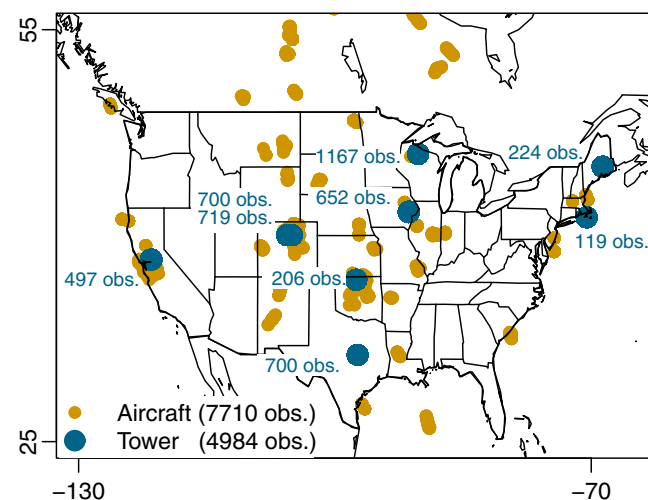
Fig. 2. CH_4 concentration measurements from 2007 and 2008 and the number of observations associated with each measurement type. Blue text lists the number of observations associated with each stationary tower measurement site.

a covariance function to describe the spatial and temporal correlation of the stochastic component and optimizes its spatial and temporal distribution simultaneously with the optimization of the activity datasets in the deterministic component (*SI Text*, Fig. S5) (26–28). Because of the stochastic component, the final emissions estimate can have a different spatial and temporal distribution from any combination of the activity data.

If the observation network is sensitive to a broad array of different source sectors and/or if the spatial activity maps are effective at explaining those sources, many activity datasets will be included in the deterministic model. If the deterministic model explains the observations well, the magnitude of CH_4 emissions in the stochastic component will be small, the assignment to specific sectors will be unambiguous, and uncertainties in the emissions estimates will be small. This result is not the case here, as discussed below (see *Results*).

A number of previous studies used top-down methods to constrain anthropogenic CH_4 sources from global (29–33) to regional (13–15, 34–38) scales over North America. Most regional studies adopted one of three approaches: use a simple box model to estimate an overall CH_4 budget (14), estimate a budget using the relative ratios of different gases (15, 37–39), or estimate scaling factors for inventories by region or source type (13, 34–36). The first two methods do not usually give explicit information about geographic distribution. The last approach provides information about the geographic distribution of sources, but results hinge on the spatial accuracy of the underlying regional or sectoral emissions inventories (40).

Here, we are able to provide more insight into the spatial distribution of emissions; like the scaling factor method above, we leverage spatial information about source sectors from an existing inventory, but in addition we estimate the distribution of emissions where the inventory is deficient. We further bolster attribution of regional emissions from the energy industry using the observed correlation of CH_4 and propane, a gas not produced by biogenic processes like livestock and landfills.

Results

Spatial Distribution of CH$_4$ Emissions. Fig. 3 displays the result of the 2-y mean of the monthly CH_4 inversions and differences from the EDGAR 4.2 inventory. We find emissions for the United States that are a factor of 1.7 larger than the EDGAR inventory. The optimized emissions estimated by this study bring the model closer in line with the observations (Fig. 4, Figs. S6 and S7). Posterior emissions fit the CH_4 observations [$R^2 = 0.64$, root mean square error (RMSE) = 31 ppb] much better than EDGAR

v4.2 ($R^2 = 0.23$, RMSE = 49 ppb). Evidently, the spatial distribution of EDGAR sources is inconsistent with emissions patterns implied by the CH_4 measurements and associated footprints.

Several diagnostic measures preclude the possibility of major systematic errors in WRF–STILT. First, excellent agreement between the model and measured vertical profiles from aircraft implies little bias in modeled vertical air mixing (e.g., boundary-layer heights) (Fig. 4). Second, the monthly posterior emissions estimated by the inversion lack statistically significant seasonality (Fig. S8). This result implies that seasonally varying weather patterns do not produce detectable biases in WRF–STILT. *SI Text* discusses possible model errors and biases in greater detail.

CH_4 observations are sparse over parts of the southern and central East Coast and in the Pacific Northwest. Emissions estimates for these regions therefore rely more strongly on the deterministic component of the flux model, with weights constrained primarily by observations elsewhere. Therefore, emissions in these areas, including from coal mining, are poorly constrained (*SI Text*).

Contribution of Different Source Sectors. Only two spatial activity datasets from EDGAR 4.2 are selected through the BIC as meaningful predictors of CH_4 observations over the United States: population densities of humans and of ruminants (Table S1). Some sectors are eliminated by the BIC because emissions are situated far from observation sites (e.g., coal mining in West Virginia or Pennsylvania), making available CH_4 data insensitive to these predictors. Other sectors may strongly affect observed concentrations but are not selected, indicating that the spatial datasets from EDGAR are poor predictors for the distribution of observed concentrations (e.g., oil and natural gas extraction and oil refining). Sources from these sectors appear in the stochastic component of the GIM (*SI Text*).

The results imply that existing inventories underestimate emissions from two key sectors: ruminants and fossil fuel extraction and/or processing, discussed in the remainder of this section.

We use the optimized ruminant activity dataset to estimate the magnitude of emissions with spatial patterns similar to animal husbandry and manure. Our corresponding US budget of 12.7 ± 5.0 TgC·y^{-1} is nearly twice that of EDGAR and EPA (6.7 and 7.0, respectively). The total posterior emissions estimate over the northern plains, a region with high ruminant density but little fossil fuel extraction, further supports the ruminant estimate (Nebraska, Iowa, Wisconsin, Minnesota, and South Dakota). Our total budget for this region of 3.4 ± 0.7 compares with 1.5 TgC·y^{-1} in EDGAR. Ruminants and agriculture may also be
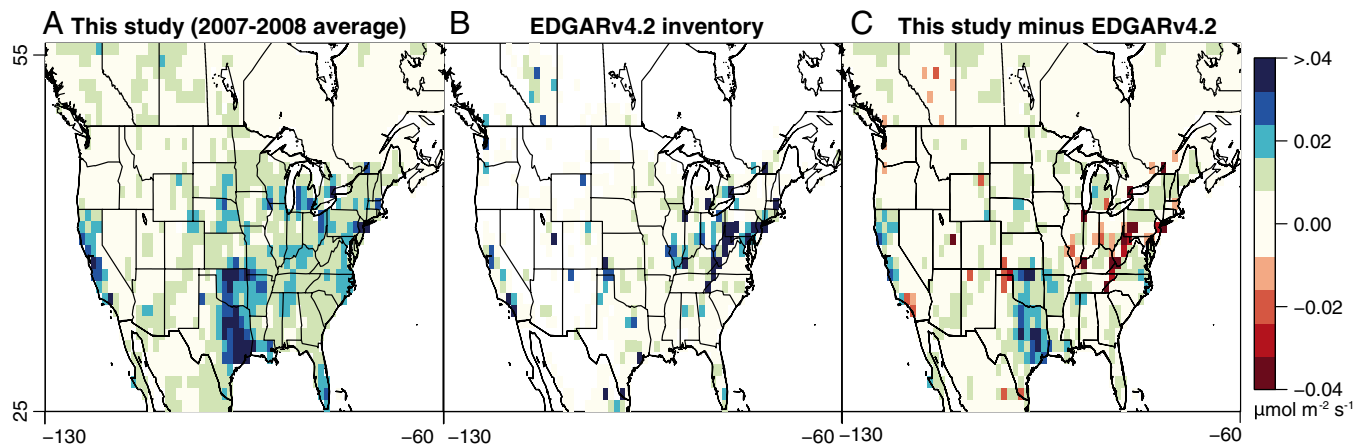

Fig. 3. The 2-y averaged CH_4 emissions estimated in this study (*A*) compared against the commonly used EDGAR 4.2 inventory (*B* and *C*). Emissions estimated in this study are greater than in EDGAR 4.2, especially near Texas and California.
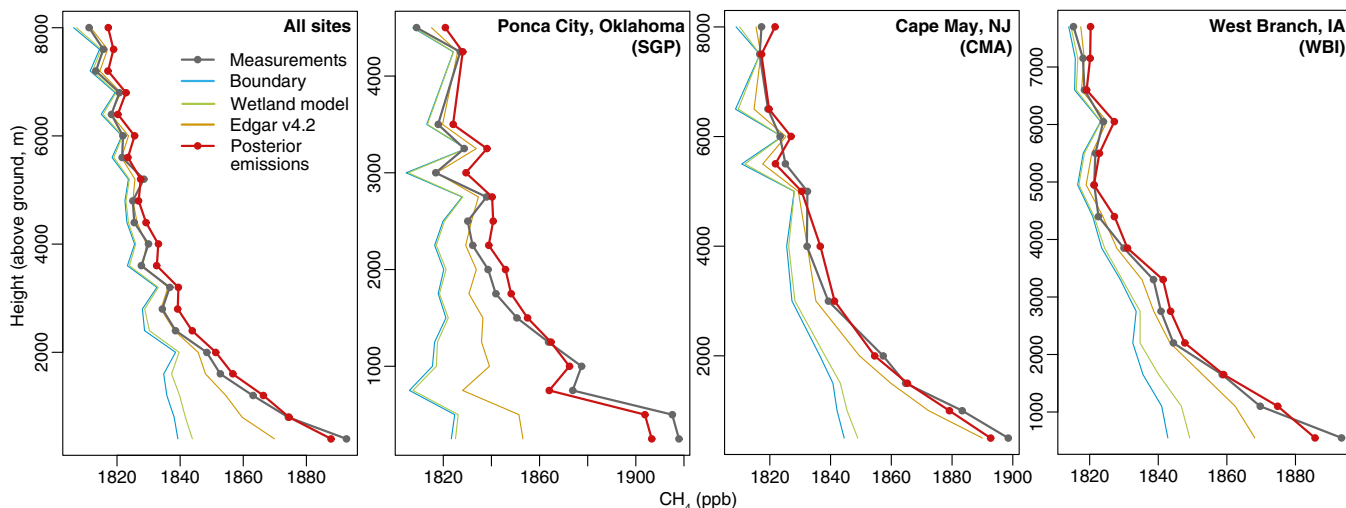
Fig. 4. A model–measurement comparison at several regular NOAA/DOE aircraft monitoring sites (averaged over 2007–2008). Plots include the measurements; the modeled boundary condition; the summed boundary condition and wetland contribution (from the Kaplan model); and the summed boundary, wetland, and anthropogenic contributions (from EDGAR v4.2 and the posterior emissions estimate).

partially responsible for high emissions over California (41). EDGAR activity datasets are poor over California (42), but several recent studies (34, 36–38, 41) have provided detailed top-down emissions estimates for the state using datasets from state agencies.

Existing inventories also greatly underestimate CH_4 sources from the south-central United States (Fig. 3). We find the total CH_4 source from Texas, Oklahoma, and Kansas to be 8.1 ± 0.96 $TgC \cdot y^{-1}$, a factor of 2.7 higher than the EDGAR inventory. These three states alone constitute $\sim 24 \pm 3\%$ of the total US anthropogenic CH_4 budget or 3.7% of net US greenhouse gas emissions [in CO_2 equivalents (10)].

Texas and Oklahoma were among the top five natural gas producing states in the country in 2007 (18), and aircraft observations of alkanes indicate that the natural gas and/or oil industries play a significant role in regional CH_4 emissions. Concentrations of propane (C_3H_8), a tracer of fossil hydrocarbons (43), are strongly correlated with CH_4 at NOAA/DOE aircraft monitoring locations over Texas and Oklahoma ($R^2 = 0.72$) (Fig. 5). Correlations are much weaker at other locations in North America ($R^2 = 0.11$ to 0.64).

We can obtain an approximate CH_4 budget for fossil-fuel extraction in the region by subtracting the optimized contributions associated with ruminants and population from the total emissions. The residual (Fig. S4C) represents sources that have spatial patterns not correlated with either human or ruminant density in EDGAR. Our budget sums to 3.7 ± 2.0 $TgC \cdot y^{-1}$, a factor of 4.9 ± 2.6 larger than oil and gas emissions in EDGAR v4.2 (0.75 $TgC \cdot y^{-1}$) and a factor of 6.7 ± 3.6 greater than EDGAR sources from solid waste facilities (0.55 $TgC \cdot y^{-1}$), the two major sources that may not be accounted for in the deterministic component. The population component likely captures a portion of the solid waste sources so this residual methane budget more likely represents natural gas and oil emissions than landfills. SI Text discusses in detail the uncertainties in this sector-based emissions estimate. We currently do not have the detailed, accurate, and spatially resolved activity data (fossil fuel extraction and processing, ruminants, solid waste) that would provide more accurate sectorial attribution.

Katzenstein et al. (2003) (14) were the first to report large regional emissions of CH_4 from Texas, Oklahoma, and Kansas; they cover an earlier time period (1999–2002) than this study. They used a box model and 261 near-ground CH_4 measurements taken over 6 d to estimate a total Texas–Oklahoma–Kansas CH_4 budget (from all sectors) of 3.8 ± 0.75 $TgC \cdot y^{-1}$. We revise their
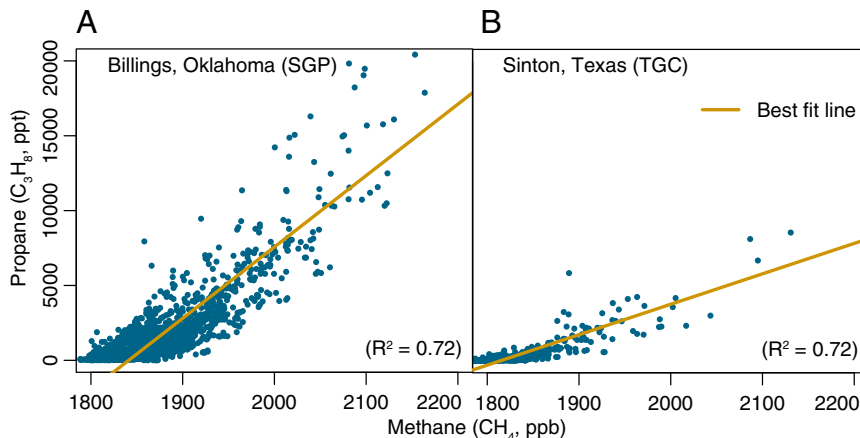

Fig. 5. Correlations between propane and CH_4 at NOAA/DOE aircraft observation sites in Oklahoma (*A*) and Texas (*B*) over 2007–2012. Correlations are higher in these locations than at any other North American sites, indicating large contributions of fossil fuel extraction and processing to CH_4 emitted in this region.

estimate upward by a factor of two based on the inverse model and many more measurements from different platforms over two full years of data. *SI Text* further compares the CH_4 estimate in Katzenstein et al. and in this study.

Discussion and Summary

This study combines comprehensive atmospheric data, diverse datasets from the EDGAR inventory, and an inverse modeling framework to derive spatially resolved CH_4 emissions and information on key source sectors. We estimate a mean annual US anthropogenic CH_4 budget for 2007 and 2008 of 33.4 ± 1.4 TgC·y^{-1} or ~7–8% of the total global CH_4 source. This estimate is a factor of 1.5 and 1.7 larger than EPA and EDGAR v4.2, respectively. CH_4 emissions from Texas, Oklahoma, and Kansas alone account for 24% of US methane emissions, or 3.7% of the total US greenhouse gas budget.

The results indicate that drilling, processing, and refining activities over the south-central United States have emissions as much as 4.9 ± 2.6 times larger than EDGAR, and livestock operations across the US have emissions approximately twice that of recent inventories. The US EPA recently decreased its CH_4 emission factors for fossil fuel extraction and processing by 25–30% (for 1990–2011) (10), but we find that CH_4 data from across North America instead indicate the need for a larger adjustment of the opposite sign.

1. Butler J (2012) The NOAA annual greenhouse gas index (AGGI). Available at http://www.esrl.noaa.gov/gmd/aggi/. Accessed November 4, 2013.
2. Fiore AM, et al. (2002) Linking ozone pollution and climate change: The case for controlling methane. *Geophys Res Lett* 29:1919.
3. Jacob D (1999) *Introduction to Atmospheric Chemistry* (Princeton Univ Press, Princeton).
4. Mitchell LE, Brook EJ, Sowers T, McConnell JR, Taylor K (2011) Multidecadal variability of atmospheric methane, 1000-1800 CE. *J Geophys Res Biogeosci* 116:G02007.
5. Dlugokencky EJ, et al. (2009) Observational constraints on recent increases in the atmospheric CH_4 burden. *Geophys Res Lett* 36:L18803.
6. Sussmann R, Forster F, Rettinger M, Bousquet P (2012) Renewed methane increase for five years (2007-2011) observed by solar FTIR spectrometry. *Atmos Chem Phys* 12:4885–4891.
7. Kirschke S, et al. (2013) Three decades of global methane sources and sinks. *Nat Geosci* 6:813–823.
8. Wang JS, et al. (2004) A 3-D model analysis of the slowdown and interannual variability in the methane growth rate from 1988 to 1997. *Global Biogeochem Cycles* 18:GB3011.
9. Ciais P, et al. (2013) *Carbon and Other Biogeochemical Cycles: Final Draft Underlying Scientific Technical Assessment* (IPCC Secretariat, Geneva).
10. US Environmental Protection Agency (2013) *Inventory of U.S. Greenhouse Gas Emissions and Sinks: 1990–2011, Technical Report EPA 430-R-13-001* (Environmental Protection Agency, Washington).
11. Olivier JGJ, Peters J (2005) CO_2 from non-energy use of fuels: A global, regional and national perspective based on the IPCC Tier 1 approach. *Resour Conserv Recycling* 45:210–225.
12. European Commission Joint Research Centre, Netherlands Environmental Assessment Agency (2010) *Emission Database for Global Atmospheric Research (EDGAR)*, Release Version 4.2. Available at http://edgar.jrc.ec.europa.eu. Accessed November 4, 2013.
13. Kort EA, et al. (2008) Emissions of CH_4 and N_2O over the United States and Canada based on a receptor-oriented modeling framework and COBRA-NA atmospheric observations. *Geophys Res Lett* 35:L18808.
14. Katzenstein AS, Doezema LA, Simpson IJ, Blake DR, Rowland FS (2003) Extensive regional atmospheric hydrocarbon pollution in the southwestern United States. *Proc Natl Acad Sci USA* 100(21):11975–11979.
15. Pétron G, et al. (2012) Hydrocarbon emissions characterization in the Colorado Front Range: A pilot study. *J Geophys Res Atmos* 117:D04304.
16. Karion A, et al. (2013) Methane emissions estimate from airborne measurements over a western United States natural gas field. *Geophys Res Lett* 40:4393–4397.
17. Howarth RW, Santoro R, Ingraffea A (2011) Methane and the greenhouse-gas footprint of natural gas from shale formations. *Clim Change* 106:679–690.
18. US Energy Information Administration (2013) *Natural Gas Annual 2011*, Technical report (US Department of Energy, Washington).
19. National Research Council (2010) *Verifying Greenhouse Gas Emissions: Methods to Support International Climate Agreements* (National Academies Press, Washington).
20. Dlugokencky EJ, Nisbet EG, Fisher R, Lowry D (2011) Global atmospheric methane: Budget, changes and dangers. *Philos Trans A Math Phys Eng Sci* 369(1943):2058–2072.
21. Lin JC, et al. (2003) A near-field tool for simulating the upstream influence of atmospheric observations: The Stochastic Time-Inverted Lagrangian Transport (STILT) model. *J Geophys Res Atmos* 108(D16):4493.
22. Nehrkorn T, et al. (2010) Coupled Weather Research and Forecasting-Stochastic Time-Inverted Lagrangian Transport (WRF-STILT) model. *Meteorol Atmos Phys* 107:51–64.
23. NOAA ESRL (2013) *Carbon Cycle Greenhouse Gas Group Aircraft Program.* Available at http://www.esrl.noaa.gov/gmd/ccgg/aircraft/index.html. Accessed November 4, 2013.
24. Biraud SC, et al. (2013) A multi-year record of airborne CO_2 observations in the US southern great plains. *Atmos Meas Tech* 6:751–763.
25. Pan LL, et al. (2010) The Stratosphere-Troposphere Analyses of Regional Transport 2008 Experiment. *Bull Am Meteorol Soc* 91:327–342.
26. Kitanidis PK, Vomvoris EG (1983) A geostatistical approach to the inverse problem in groundwater modeling (steady state) and one-dimensional simulations. *Water Resour Res* 19:677–690.
27. Michalak A, Bruhwiler L, Tans P (2004) A geostatistical approach to surface flux estimation of atmospheric trace gases. *J Geophys Res Atmos* 109(D14):D14109.
28. Gourdji SM, et al. (2012) North American CO_2 exchange: Inter-comparison of modeled estimates with results from a fine-scale atmospheric inversion. *Biogeosciences* 9:457–475.
29. Chen YH, Prinn RG (2006) Estimation of atmospheric methane emissions between 1996 and 2001 using a three-dimensional global chemical transport model. *J Geophys Res Atmos* 111(D10):D10307.
30. Meirink JF, et al. (2008) Four-dimensional variational data assimilation for inverse modeling of atmospheric methane emissions: Analysis of SCIAMACHY observations. *J Geophys Res Atmos* 113(D17):D17301.
31. Bergamaschi P, et al. (2009) Inverse modeling of global and regional CH4 emissions using SCIAMACHY satellite retrievals. *J Geophys Res Atmos* 114(D22):D22301.
32. Bousquet P, et al. (2011) Source attribution of the changes in atmospheric methane for 2006-2008. *Atmos Chem Phys* 11:3689–3700.
33. Monteil G, et al. (2011) Interpreting methane variations in the past two decades using measurements of CH_4 mixing ratio and isotopic composition. *Atmos Chem Phys* 11:9141–9153.
34. Zhao C, et al. (2009) Atmospheric inverse estimates of methane emissions from central California. *J Geophys Res Atmos* 114(D16):D16302.
35. Kort EA, et al. (2010) Atmospheric constraints on 2004 emissions of methane and nitrous oxide in North America from atmospheric measurements and receptor-oriented modeling framework. *J Integr Environ Sci* 7:125–133.
36. Jeong S, et al. (2012) Seasonal variation of CH_4 emissions from central California. *J Geophys Res* 117:D11306.
37. Peischl J, et al. (2012) Airborne observations of methane emissions from rice cultivation in the Sacramento Valley of California. *J Geophys Res Atmos* 117(D24):D00V25.
38. Wennberg PO, et al. (2012) On the sources of methane to the Los Angeles atmosphere. *Environ Sci Technol* 46(17):9282–9289.
39. Miller JB, et al. (2012) Linking emissions of fossil fuel CO2 and other anthropogenic trace gases using atmospheric 14CO2. *J Geophys Res Atmos* 117(D8):D08302.
40. Law RM, Rayner PJ, Steele LP, Enting IG (2002) Using high temporal frequency data for CO_2 inversions. *Global Biogeochem Cycles* 16(4):1053.
41. Jeong S, et al. (2013) A multitower measurement network estimate of California's methane emissions. *J Geophys Res Atmos*, 10.1002/jgrd.50854.
42. Xiang B, et al. (2013) Nitrous oxide (N2O) emissions from California based on 2010 CalNex airborne measurements. *J Geophys Res Atmos* 118(7):2809–2820.
43. Koppmann R (2008) *Volatile Organic Compounds in the Atmosphere* (Wiley, Singapore).